Applied Surface Science 418 (2017) 388–392

Contents lists available at ScienceDirect

Applied Surface Science

journal homepage: www.elsevier.com/locate/apsusc

Full Length Article

# Studies on interface between $In_2O_3$ and $CuInTe_2$ thin films

M.R. Ananthan[a,b,*], P. Malar[c,d], Thomas Osipowicz[c], S. Kasiviswanathan[a]

[a] Thin Films Laboratory, Department of Physics, Indian Institute of Technology Madras, Chennai, 600 036, India
[b] Department of Physics, Karpagam College of Engineering, Coimbatore, India
[c] Centre for Ion Beam Applications, Department of Physics, National University of Singapore, Singapore
[d] Research Institute, Department of Physics and Nanotechnology, SRM University, Chennai, India

ARTICLE INFO

*Article history:*
Received 28 September 2016
Received in revised form
10 December 2016
Accepted 15 December 2016
Available online 16 December 2016

*Keywords:*
$CuInTe_2$
$In_2O_3$
Thin film interface
Rutherford backscattering spectrometry
Raman spectroscopy

ABSTRACT

Interface between dc sputtered $In_2O_3$ and stepwise flash evaporated $CuInTe_2$ films were studied by probing $Si/In_2O_3/CuInTe_2$ and $Si/CuInTe_2/In_2O_3$ structures with the help of glancing angle X-ray diffraction, Rutherford backscattering spectrometry and micro-Raman spectroscopy. The results showed that in $Si/In_2O_3/CuInTe_2$ structure, a ~20 nm thick interface consisting of In, Cu and O had formed between $In_2O_3$ and $CuInTe_2$ and was attributed to the diffusion of Cu from $CuInTe_2$ into $In_2O_3$ film. On the other hand, in $Si/CuInTe_2/In_2O_3$ structure, homogeneity of the underlying $CuInTe_2$ film was found lost completely. An estimate of the masses of the constituent elements showed that the damage was caused by loss of Te from $CuInTe_2$ film during the growth of $In_2O_3$ film on $Si/CuInTe_2$.



## 1. Introduction

Thin film solar cells with I-III-$VI_2$ film as absorber layer, Mo film deposited on glass substrate serves as back electrode, with the glass plate providing the necessary mechanical strength. An alternate approach [1–3] to the back metallic contact is to replace Mo film with a transparent conducting oxide (TCO) film. An important advantage [3] of using TCO electrodes is that, apart from providing electrical contact, they can transmit unabsorbed portions of the incident radiation, as TCO's have an average transmittance of about 85% in the visible and near infrared regions. Solar cells with TCO back contact are sometimes termed as bifacial [3], as it is possible to illuminate from both sides and therefore forms the basic unit of multi-junction or tandem solar cells. The bifacial structures are commonly visualized in two different forms: a) the conventional form in which the cell is developed by first forming the back contact TCO on the glass plate and b) the "inverted" structure in which the back contact is deposited last. The latter structure is called "superstrate" type cell. Two major factors [3,4] that affect the performance of the solar cells with TCO back contact are 1) changes in the structural and phase homogeneity of the absorber and the TCO films, 2) interface layers, if any, formed between TCO and absorber films due to chemical reaction or inter-diffusion across the interface. For instance, any change in the characteristics of the TCO increases the series resistance and reduce the transmitted light, which in turn will affect the other cells that are in tandem. Therefore, application of TCO as back contact necessitates a detailed prior study of interface between chalcopyrite and TCO thin films.

The present work deals with probing of the interface formed between stepwise flash evaporated $CuInTe_2$ films and dc sputtered $In_2O_3$ films using Rutherford backscattering spectrometry (RBS), glancing angle X-ray diffraction (GXRD) and micro-Raman spectroscopy. $CuInTe_2$ belongs to the chalcopyrite ternary compound semiconductor family of compounds and exhibits characteristics displayed by good solar radiation absorber materials. On the other hand, $In_2O_3$ is a wide band gap semiconductor (band gap ~3.75 eV) with an average optical transmittance of ~85% in the visible region [5]. Stoichiometric $In_2O_3$ shows semi-insulating characteristics [6], however, it becomes a degenerate n-type semiconductor with metallic characteristics in oxygen deficient form. It is apparent that the function of $In_2O_3$, when it is in contact with other materials variable from buffer to Ohmic contact by controlling the oxygen vacancies alone.

In order to probe the interfaces, two types of structures, viz., $Si/In_2O_3/CuInTe_2$ and $Si/CuInTe_2/In_2O_3$ have been formed. The interface formed between $In_2O_3$ and $CuInTe_2$ in the former is analogous to the TCO-chalcopyrite interface in absorber based solar cells

* Corresponding author at: Department of Physics, Karpagam College of Engineering, Coimbatore, Tamil Nadu, India.
*E-mail addresses:* ananthan@kce.ac.in, mrananthan@gmail.com (M.R. Ananthan).

http://dx.doi.org/10.1016/j.apsusc.2016.12.124
0169-4332/

with TCO back contact [3] as $CuInTe_2$ is deposited on $In_2O_3$ film. On the other hand, the interface between $In_2O_3$ and $CuInTe_2$ thin films in the latter structure is similar to the chalcopyrite-TCO interface in "superstrate" type solar cells with TCO Ohmic contact [1,3]. Since, the order in which $In_2O_3$ and $CuInTe_2$ films are formed and the methods used for depositing the two are different, there is a possibility that interface characteristics differ.

## 2. Experiments

$CuInTe_2$ and $In_2O_3$ films were grown by step wise flash evaporation method and dc reactive sputtering respectively. The details of growth of $CuInTe_2$ and $In_2O_3$ thin films were presented elsewhere [7,8]. Briefly, $CuInTe_2$ films were grown onto substrates held at 573 K using step wise flash evaporation. $In_2O_3$ thin films were grown by direct current reactive sputtering technique using indium target of 5N purity in the presence of 2% of $O_2$ and Ar mixture. Sputtering was done at a constant power of 100 W and at a base pressure of $\sim 5 \times 10^{-2}$ mbar. HF cleaned Si (100) wafers were used as substrates. In order to form $Si/In_2O_3/CuInTe_2$ structure, $In_2O_3$ film was first deposited on Si, followed by $CuInTe_2$ film. $In_2O_3$ and $CuInTe_2$ films were grown in separate thin film units. $Si/CuInTe_2/In_2O_3$ structure was fabricated by first depositing $CuInTe_2$ on Si, followed by $In_2O_3$ film.

GXRD studies were made using filtered $CuK_\alpha$ radiation in a PANalytical model X'Pert PRO XRD unit. All the measurements were recorded using a glancing angle of 3° (with the sample surface), which was chosen such that the signal strength from the Si wafer was small compared to those from the films. RBS measurements were made using the 3.5 MV Singletron Accelerator at the Centre for Ion Beam Applications at National University of Singapore. A 2 MeV $He^+$ beam of typically 20 nA beam current and 1 $mm^2$ spot size was used. RBS spectra were recorded with a planar silicon detector of 16 keV energy resolution and at 160° scattering angle, in the IBM geometry. RBS spectra were simulated using the simulation software "XRUMP" [9]. Micro-Raman measurements were carried out in backscattering geometry with a Horiba Jobin Yvon, model HR800 UV Raman microscope equipped with an Olympus imaging system. A 488 nm line from $Ar^+$ laser source was used as the excitation beam. The laser power used for measurements was about 60 μW and the beam diameter was about 5 μm.

## 3. Results and discussion

### 3.1. GXRD studies

Typical GXRD patterns of $Si/In_2O_3/CuInTe_2$ and $Si/CuInTe_2/In_2O_3$ recorded with a glancing angle of 3° are displayed in Fig. 1a and b respectively. Analysis of the pattern shown in Fig. 1a revealed the reflections are from the different planes of $CuInTe_2$ and $In_2O_3$ films indicating that both are homogeneous. Peaks corresponding to $In_2O_3$ are prefixed as INO. In Fig. 1a, reflections from $CuInTe_2$ thin film dominate the pattern as it forms the top layer. On the other hand, the pattern shown in Fig. 1b does not contain peaks expected for $CuInTe_2$ and all the peaks except one that is marked 'X' are identified to match with $In_2O_3$ standard data. The absence of any reflections corresponding to $CuInTe_2$ indicate that either the diffracted signals from $CuInTe_2$ thin film are too weak to contribute or the film itself is altered during the deposition of $In_2O_3$. The constituent elements (Cu, In & Te) or oxides of the elements or the binaries ($Cu_2Te$ and $In_2Te_3$) is attributed to contribute to the unidentified peak, marked X, appearing at a 2θ value of ~32.88 deg. Planes that have 2θ values close to ~32.88 deg are (101) plane of In (relative intensity 100% with 2θ = 32.965 deg; JCPDS card no.: 005–0642) and (210) plane

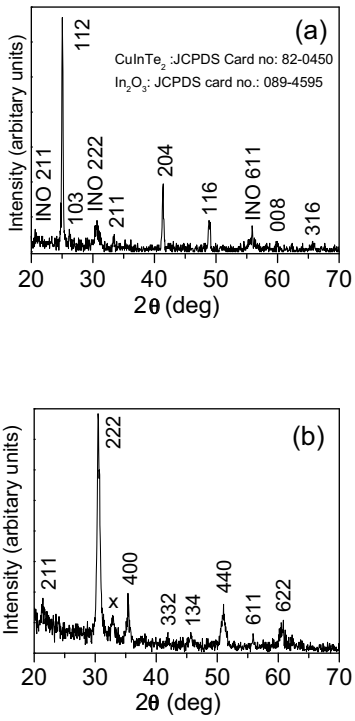


**Fig. 1.** GXRD pattern of (a) $Si/In_2O_3/CuInTe_2$ and (b) $Si/CuInTe_2/In_2O_3$ structures recorded at an angle of 3°. In panel (a) reflections from $In_2O_3$ are prefixed with INO. The peak marked X in panel (b) is due to In (101) reflection.

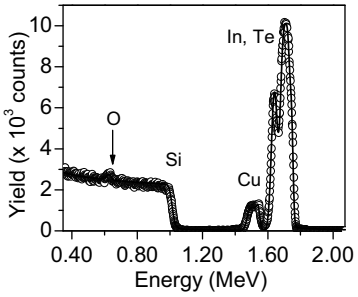


**Fig. 2.** RBS spectrum of $Si/In_2O_3/CuInTe_2$ structure. The edges due to various elements are indicated for convenience. The arrow shows the peak due to oxygen.

of $TeO_2$ (relative intensity 45% with 2θ = 32.778 deg; JCPDS card no.:009–0433). The presence of $In_2O_3$ reflections and absence of $CuInTe_2$ reflections in the GXRD pattern of $Si/CuInTe_2/In_2O_3$ confirm the damage of underlying $CuInTe_2$ during the DC reactive sputtered growth of top $In_2O_3$ film.

### 3.2. RBS studies

#### 3.2.1. $Si/In_2O_3/CuInTe_2$ structure

RBS measurements were made to analyze and determine the composition, thickness and interface integrity of the multilayer structures. Fig. 2 shows a typical RBS spectrum of $Si/In_2O_3/CuInTe_2$ structure. The experimental data points and the simulated curve are denoted by symbols and continuous line respectively. The spectrum consists of superimposed yields of In from $In_2O_3$ as well as $CuInTe_2$, Te and Cu from $CuInTe_2$. Oxygen from $In_2O_3$ is seen as superimposed yield on the Si plateau and is indicated by an arrow. The simulation that reproduced the experimental data of $Si/In_2O_3/CuInTe_2$ structure showed that the structure consists of five layers including the substrate. The top $CuInTe_2$ film is found to be slightly Te rich with a thickness of ~102 nm. The atomic percent-

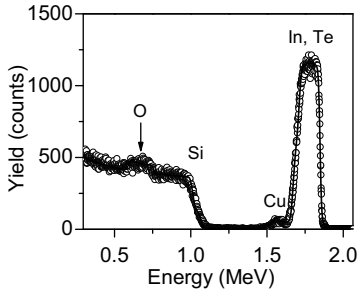


**Fig. 3.** RBS spectrum of $Si/CuInTe_2/In_2O_3$ structure.

ages of the constituent elements viz., Cu, In and Te were found to be 24.3, 24.8 and 50.9 respectively. The interface between $CuInTe_2$ and $In_2O_3$ films was not sharp. The interface contained a ~20 nm thick inhomogeneous region consisting of Cu, In and O, the atomic percentages of which were found to be 1.0, 40.4 and 58.6 respectively. The elemental concentration suggests that the interface region consists of mainly oxygen deficient $In_2O_3$ with slight Cu diffusion from the top $CuInTe_2$ film. This is consistent with the elemental analysis of the top $CuInTe_2$ film which showed copper deficiency. Earlier studies [8] on $CuInSe_2/In_2O_3$ interfaces have exhibited similar Cu diffusion, which is facilitated by the high self diffusion coefficient of Cu in $CuInSe_2$. Cu diffusion has also been observed in other structures such as $CuInSe_2$/CdS [10] and $CuGaSe_2$/ZnO [11], though under different processing conditions. The third layer was found to consist of ~37 nm thick oxygen deficient $In_2O_3$ film having atomic percentages of In and O as 40.8 and 59.2 respectively. The fourth layer was an inhomogeneous intermediate layer of ~25 nm in thickness formed between $In_2O_3$ film and Si. It consists of In, O and Si with atomic percentages 11.2, 32.3 and 56.5 respectively. The formation of an interface region between Si and DC sputtered $In_2O_3$ thin films have been reported [12] and is attributed to the high energy secondary electrons striking the Si surface during the initial stages of $In_2O_3$ film growth.

### 3.2.2. *Si/CuInTe$_2$/In$_2$O$_3$ structure*

Fig. 3 shows a typical RBS spectrum of $Si/CuInTe_2/In_2O_3$ structure with the experimental and simulated curve being denoted by symbols and continuous line respectively. It is of interest to compare Fig. 3 with Fig. 2, which shows the RBS spectra of $Si/In_2O_3/CuInTe_2$ structure. The yield due to O appearing as superimposed peak (indicated by an arrow) on the Si plateau is rather broad, which points to the presence of thick region containing O. The simulations initiated with the configuration $Si/CuInTe_2/In_2O_3$ were far from reproducing the experimental data. For instance, the leading edge of the spectra on the high energy should be due to In yield, but showed signs of yield from Te as well.

The simulated spectra that reproduced the experimental data revealed the presence of four different layers with different thicknesses, in addition to the Si substrate. The top layer was found to be ~90 nm thick and had Cu, In, Te and O with atomic percentages 4.2, 34.6, 2.3 and 58.9 respectively. The second layer obtained from the simulations was ~95 nm thick and consisted of the same elements that were present in the first layer. The simulations yielded the atomic percentages of Cu, In, Te and O as 6.0, 36.3, 3.6 and 54.1 respectively, which are close to those obtained for the corresponding elements in the top layer. The third layer was found to be ~85 nm thick and contained Si in addition to the elements present in the first two layers. The calculated atomic percentages of the individual elements, viz., Cu, In, Te, O and Si were 2.7, 34.9, 3.0, 41 and 17.8 respectively. The fourth layer was found to be ~50 nm thick and contained In, Si and O with atomic percentages 4.8, 33.4 and 61.8 respectively. The bottom most layer considered in the simulations was the thick Si substrate.

The following conclusions are drawn from the results of the simulations to the RBS spectra of $Si/CuInTe_2/In_2O_3$ structure. 1) During sputtering of $In_2O_3$ film over $CuInTe_2$ film, the latter gets destroyed completely, 2) The top two layers with 90 and 95 nm in thicknesses have $In_2O_3$ as the primary constituent, 3) There is outward diffusion of Si from the substrate into the third layer and 4) The fourth layer formed over Si may consist mainly of $SiO_2$.

The RBS results presented in the previous sections clearly indicate that in $Si/In_2O_3/CuInTe_2$ structure both $In_2O_3$ and $CuInTe_2$ retain their phase homogeneity but for the presence of a thin interface region due to diffusion of Cu. On the other hand, while forming the $Si/CuInTe_2/In_2O_3$ structure, the expected layer configuration is destroyed when $In_2O_3$ is being deposited. The principal reason for this may be the method used for the deposition of $In_2O_3$ thin film, viz., DC sputtering which is quite different from thermal/electron beam evaporation or DC magnetron sputtering. A critical factor is the high-energy secondary electrons in the plasma, which strike the substrate during sputtering [13]. In fact, the substrate was found to reach ~675 K (higher than the temperature (~573 K) at which the $CuInTe_2$ thin film is grown) within a minute solely due to secondary electron bombardment [8]. Further, the substrate is also subjected to constant bombardment by other high-energy species in the plasma during the film growth. Although these factors can improve the film adhesion to the substrate, they can also cause structural damage by inducing diffusion and sputtering away of the material present on the substrate. Thus, it probable that during the initial stages of $In_2O_3$ film growth, the sputtered species (charged or neutral In-O atoms/clusters) diffuse through the $CuInTe_2$ film aided by the secondary electron bombardment and the consequent heating of the substrate. The In-O clusters that reach the Si surface will be reduced to form $SiO_2$ as the Gibbs free energy data for the formation for $In_2O_3$ and $SiO_2$ [14,15,12] show that in the temperature range from 300 to 1000 K, the formation of $SiO_2$ is preferred over $In_2O_3$. Therefore, $SiO_2$ film is expected to form near the substrate.

The growth rate of $SiO_2$, however, will be reduced eventually, since the diffusivity of Si in $SiO_2$ is small [16], and formation of $In_2O_3$ will dominate. Since the $SiO_2$ grows by reduction of In-O, concentration of In should increase and a In rich transition region should be present before $In_2O_3$ growth dominates. The reduction of $In_2O_3$ at the interface and the formation of an interface region consisting In-O-Si have been observed by Malar et al. [8] in their studies on $In_2O_3$/Si interface and by de Nijs et al. [17] in their studies on μc–Si:C:H/$In_2O_3$ junctions formed by depositing μc–Si:C:H films over $In_2O_3$. Similar results have also been reported by Yang et al. [18] from their studies on the effect of annealing on Si/ITO interface.

The results of RBS studies are in concurrence with those of GXRD studies. GXRD pattern of $Si/CuInTe_2/In_2O_3$ (Fig. 1b) clearly showed $In_2O_3$ as the major phase present. This is in agreement with RBS simulations which yielded five layer structure, with top two layers (total thickness ~185 nm) having In and O as the major constituents. However, the minor elements (Cu and Te) or their oxides indicated by the RBS simulations have not been detected in GXRD. The possible reasons are that the reflections from them are weak to be observed with GXRD. Further, some of the metallic oxides have reflections, whose lattice spacings values are very close to those of $In_2O_3$. For instance, the (002) plane of CuO has peak at 35.496 deg (JCPDS card no.: 045–0937), which overlap with 35.455 deg reflection from (400) plane of $In_2O_3$. The additional peak in GXRD that appears at 32.88 deg (Fig. 1b) can be attributed to (101) peak of In (JCPDS card no.:005–0642). This is because, apart from the fact that it is the highest intensity peak of In, evidence for the presence of source of In, viz., In rich region (layer 3) has been shown by the RBS simulations.

**Table 1**
Weight of constituent elements present in individual layer.

| Layer number | Weight of individual elements in μg | | |
|---|---|---|---|
| | Cu | In | Te |
| 1 | 3.2 | 47 | 3.5 |
| 2 | 4.4 | 48.4 | 5.5 |
| 3 | 1.8 | 42.7 | 4.2 |
| 4 | – | 2.0 | – |

The disintegration of $CuInTe_2$, due to the growth of $In_2O_3$ has been interpreted as due to the diffusion of sputtered species through $CuInTe_2$ film, facilitated by the secondary electron bombardment. Bombarding species with low energy can raise the substrate temperature apart from creating defects, while those with sufficiently high energy will sputter away the substrate material, in addition. These two processes are differentiated by mass conservation considerations as sputtering should result in mass loss, while mass will be conserved if the energy of the striking species is dissipated in heat generation alone.

In the present experiments, the thickness of the $CuInTe_2$ thin film deposited on Si was ~115 nm while the expected thickness of the top $In_2O_3$ film was ~217 nm. These thicknesses were obtained from plain Si substrates kept during the depositions of $CuInTe_2$ and $In_2O_3$ respectively. The weights of the constituent elements in each layer of the $Si/CuInTe_2/In_2O_3$ and $Si/In_2O_3/CuInTe_2$ were calculated from the thicknesses and atomic compositions determined by the experiments and simulation on an assumption that the atomic density of each layer is equal to the corresponding bulk material which is tabulated in Table 1. The density of the top three layers were taken to be that of $In_2O_3$ (7.18 g $cm^{-3}$) [19], the density of the fourth layer was assumed to be that of $SiO_2$ (2.19 g $cm^{-3}$) [20]. The density of $CuInTe_2$ was taken to be 6.0 g $cm^{-3}$ [21]. Calculations were made taking a film surface area of 1 $cm^2$. The calculated mass of Cu in the first, second and third layers was respectively, 3.2, 4.4 and 1.8 μg. If there is no loss of mass, then all the Cu in the $CuInTe_2$ film should be redistributed in the top three layers. The thickness of the $CuInTe_2$ film that will contain 9.4 μg of Cu (total mass of Cu in the first three layers) is 107 nm. This value is close to the actual thickness (115 nm) of the $CuInTe_2$ film on Si. The same reasoning can be applied to check conservation of the masses of In and Te. The mass of In in the first to fourth layers was found to be, respectively 47.0, 48.4, 42.7 and 2.0 μg and the total mass (~140 μg) should have been sourced from $CuInTe_2$ and $In_2O_3$ thin films. The In mass required for forming ~107 nm thick $CuInTe_2$ film is 17.0 μg, which means the remaining mass of ~123 μg should have come during $In_2O_3$ deposition. The thickness of $In_2O_3$ film that will have about 123 μg of In is 207 nm. This value, considering the assumptions made for the calculations, is in excellent agreement with the thickness of the $In_2O_3$ film (217 nm) deposited on $CuInTe_2$ film. The mass of Te present on first, second and third layers were found to be, respectively 3.5, 5.5 and 4.1 μg. While the total Te mass present on the structure is ~13.1 μg, the mass needed to form stoichiometric $CuInTe_2$ film of thickness ~107 nm is 37.8 μg. This is in contrast to that observed in the case of Cu and In and shows that during the deposition of $In_2O_3$, there is loss of Te present in $CuInTe_2$. The amount of Te lost from $CuInTe_2$ is quite high (~60%) and is possibly due to the preferential sputtering of Te caused by the impinging species and the associated temperature rise. Recent Raman studies on laser induced changes in $CuInTe_2$ films have shown that at sufficiently high probing laser beam power, Te segregation can occur on the film surface [22]. It is to be noted that in the above considerations, the density of individual layers has been assumed to be that of homogeneous films, although the layers contained other elements as well. Therefore, the values obtained should be considered as rough estimates of the actual masses. However, loss of Te can be ascertained with confidence as the amount of Te lost is quite high and is much higher than the errors involved.

### 3.3. Raman analysis

Micro-Raman measurements were made on $Si/In_2O_3/CuInTe_2$ and $Si/CuInTe_2/In_2O_3$ structures using 60 μW 488 nm laser beam. Low laser power was chosen so that the beam does not interact with the multilayer structure. Fig. 4a and b show typical Raman spectra of $Si/In_2O_3/CuInTe_2$ and $Si/CuInTe_2/In_2O_3$ structures respectively. In Fig. 4a and b, the symbols denote the experimental data, while the continuous black and grey lines denote the overall fit and individual Lorentzians respectively.

The spectrum shown in Fig. 4a appears very similar to that of $CuInTe_2$ film deposited directly on Si [22]. Deconvolution of the spectra revealed modes expected for $CuInTe_2$, which corroborate the results of XRD and RBS measurements. On the other hand, the Raman spectrum of $Si/CuInTe_2/In_2O_3$ structure (Fig. 4b) shows two broad beaks and is otherwise featureless. Deconvolution of the spectra yielded three peaks at about 120, 140 and 163 $cm^{-1}$. The peaks that have appeared at 120 and 140 $cm^{-1}$, are associated with the $A_1$ and E modes of Te [23], since the oxides of the constituent elements do not have modes at these frequencies. The appearance of modes due to Te in the Raman spectra indicates the presence of elemental Te. It is surprising to note that Raman spectra are dominated by Te modes though there is about 60% loss of Te. This is due to the high absorption coefficient of Te at 488 nm [24]. Signals from segregated Te have been found to dominate the Raman spectra of bulk and thin films $CuInTe_2$ subjected to laser irradiation, the details of which have already been presented in our previous studies [22].

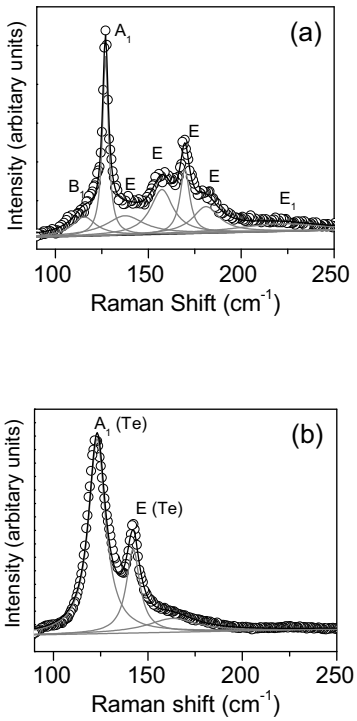


**Fig. 4.** Raman spectra of (a) $Si/In_2O_3/CuInTe_2$ and (b) $Si/CuInTe_2/In_2O_3$ structures. The symbols, grey lines and the black line through the data points represent, respectively the experimental data, individual Lorenzians and the overall fit.

## 4. Conclusion

The interface between dc sputtered $In_2O_3$ and $CuInTe_2$ thin films have been studied by analyzing $Si/In_2O_3/CuInTe_2$ and $Si/CuInTe_2/In_2O_3$ structures using GXRD, RBS and Raman spectroscopy. The results show $In_2O_3$ and $CuInTe_2$ films have retained their homogeneity in the former structure but for the presence of a thin inhomogeneous interface region, whereas in the latter structure $CuInTe_2$ film has been completely destroyed. The destruction of $CuInTe_2$ film is attributed to the striking of the substrate ($Si/CuInTe_2$) by high energy secondary electrons and other species during the DC sputter deposition of $In_2O_3$ and the subsequent loss of Te.

## References


[1] M.D. Heinemann, F. Ruske, D. Greiner, A.R. Jeong, M. Rusu, B. Rech, R. Schlatmann, C.A. Kaufmann, Advantageous light management in $Cu(In,Ga)Se_2$ superstrate solar cells, Sol. Energy Mater. Sol. Cells 150 (2016) 76–81.

[2] T. Nakada, Y. Hirabayashi, T. Tokado, D. Ohmori, T. Mise, Novel device structure for $Cu(In,Ga)Se_2$ thin film solar cells using transparent conducting oxide back and front contacts, Sol. Energy 77 (2004) 739–747.

[3] T. Nakada, Microstructural and diffusion properties of CIGS thin film solar cells fabricated using transparent conducting oxide back contacts, Thin Solid Films 480–481 (2005) 419–425.

[4] P. Xin, J.K. Larsen, F. Deng, W.N. Shafarman, Development of $Cu(In,Ga)Se_2$ superstrate devices with alternative buffer layers, Sol. Energy Mater. Sol. Cells 157 (2016) 85–92.

[5] I. Hamberg, C.G. Granquist, Evaporated Sn-doped $In_2O_3$ films: basic optical properties and applications to energy-efficient windows, J. Appl. Phys. 60 (2005) R123–R159.

[6] S. Kasiviswanathan, G. Rangarajan, Direct current magnetron sputtered $In_2O_3$ films as tunnel barriers, J. Appl. Phys. 75 (1994) 2572–2577.

[7] M.R. Ananthan, S. Kasiviswanthan, Growth and characterization of stepwise flash evaporated $CuInTe_2$ thin films, Sol. Energy Mater. Sol. Cells 93 (2009) 188–192.

[8] P. Malar, B.C. Mohanty, S. Kasiviswanathan, Characterization of interface between $CuInSe_2$ and $In_2O_3$, J. Phys. Chem. Solids 66 (2005) 1928–1932.

[9] L. Doolittle, Algorithms for the rapid simulation of Rutherford backscattering spectra, Nucl. Instrum. Methods B 9 (1985) 344–351.

[10] Y.L. Soo, S. Huang, Y.H. Kao, S.K. Deb, K. Ramanathan, T. Takizawa, Migration of constituent atoms and interface morphology in a heterojunction between CdS and $CuInSe_2$ single crystals, J. Appl. Phys. 86 (1999) 6052–6058.

[11] F.J. Haug, M. Krejci, H. Zogg, A.N. Tiwari, M. Kirsch, S. Siebentritt, Characterization of $CuGa_xSe_y$/ZnO for superstrate solar cells, Thin Solid Films 361–362 (2000) 239–242.

[12] P. Malar, B.C. Mohanty, S. Kasiviswanathan, Growth and Rutherford backscattering spectrometry study of direct current sputtered indium oxide films, Thin Solid Films 488 (2005) 26–33.

[13] D.J. Ball, Plasma diagnostics and energy transport of a dc discharge used for sputtering, J. Appl. Phys. 43 (1972) 3047–3057.

[14] I. Barin, Thermochemical Data of Pure Substances, vol. I&II, VCH Weinheim, Germany, 1989, pp. 716–717, pp. 1359–1360.

[15] O. Knacke, O. Kubaschewski, K. Hesselmann (Eds.), Thermochemical Properties of Inorganic Substances, vol. I&II, Springer-Verlag, Berlin, 1991, pp. 1835–1839, p. 925.

[16] R. Beyers, Thermodynamic considerations in refractory metal-silicon-oxygen systems, J. Appl. Phys. 56 (1984) 147–152.

[17] J.M.M. de Nijs, R.K.G.M. Aarts, Study of the reduced $In_2O_3$/μc-Si:H interface by means of factor analysis, Surf. Interf. Anal. 17 (1991) 628–634.

[18] C. Yang, W. Ow, Y. Shigesato, D.C. Paine, Interfacial stability of an indium tin oxide thin film deposited on Si and $Si_{0.85}Ge_{0.15}$, J. Appl. Phys. 88 (2000) 3717–3723.

[19] P. Walker, W.H. Tarn, CRC Hand Book of Metal Etchants, CRC Press LLC, Boca Raton, 1990, pp. 675.

[20] J.F. Shackelford, W. Alexander, CRC Materials Science and Engineering Hand Book, Third edn., CRC Press LLC, Boca Roton, 2001, pp. 83.

[21] J.L. Shay, J.H. Wernick, Ternary Chalcopyrite Semiconductors: Growth, Electronic Properties and Applications, Pergamon Press, Oxford, 1975.

[22] M.R. Ananthan, Bhaskar Chandra Mohanty, S. Kasiviswanathan, Micro-Raman spectroscopy studies of bulk and thin films of $CuInTe_2$, Semicond. Sci. Technol. 24 (2009) 075019.

[23] A.S. Pine, G. Dresselhaus, Raman spectra and lattice dynamics of tellurium, Phys. Rev. B 2 (1971) 356–371.

[24] V.V. Artamonov, M.Y. Valakh, V.V. Strelchuk, A. Baidullaeva, P.E. Mozol, Raman scattering by tellurium films on CdTe single crystals, J. Appl. Spectrosc. 48 (1988) 653–655.